Medical Hypotheses 175 (2023) 111081

Contents lists available at ScienceDirect

Medical Hypotheses

journal homepage: www.elsevier.com/locate/mehy

Determination of the effect of silica nanoparticles on TRP currents in retinal pigment epithelial cells by entropy measurement

Fatma Söğüt [a], Mahmut Akıllı [b,d], Ayşe Hümeyra Kaynar [c], Handan Tuncel [d], Deniz Kibar [e], Şakir Necat Yılmaz [e], Ülkü Çömelekoglu [c,*]

[a] Vocational School of Health Service, Mersin University, Mersin, Turkey
[b] Medical Imaging Techniques Program, Vocational School, Arel University, İstanbul, Turkey
[c] Department of Biophysics, Faculty of Medicine, Mersin University, Mersin, Turkey
[d] Department of Biophysics, Cerrahpaşa Faculty of Medicine, Istanbul University-Cerrahpaşa, İstanbul, Turkey
[e] Department of Histology-Embryology, Faculty of Medicine, Mersin University, Mersin, Turkey

ARTICLE INFO

Keywords:
Retinal pigment epithelium
Nanoparticle
Ion channel
Whole cell recording
TRP channel
Entropy

ABSTRACT

Ion channels in cell membranes are gated, water-filled pores that allow passive transport of ions across the membrane along their electrochemical gradient. Recent studies have shown that nanoparticles can interact with ion channels and change their currents kinetics properties of the channel. In this study, we used the transient receptor potential (TRP) channel currents in retinal pigment epithelial (RPE) cells recorded by whole-cell patch clamp technique to observe the silica nanoparticle-ion channel interaction. For whole cell recordings, we clamped membrane potential to −40 mV and used a ramp of 1000 ms duration for stimulation. The ramp was increased from −140 mV to +60 mV. We used windowed scalogram entropy and compared the results with windowed scale index method. Our results indicated that the temporal change of entropy using windowed scalogram entropy method is sensitive to demonstrating the effect of silica nanoparticles on RPE cell TRP currents. Furthermore, windowed scale index can analyze the temporal fluctuations in the aperiodicity of cell membrane current signals. Our findings suggest that entropy measurement methods may be useful in the function analysis of cell ion channels.

Introduction

Ion channels are integral proteins embedded in the phospholipid bilayer of cell membranes. The hydrophobic parts of the channel protein can come into contact with the phospholipid molecules of the membrane, while the hydrophilic parts resemble a water-filled pore. Ion channels can allow one ion to pass but not another ion. That is, it is selectively permeable. The most characteristic physical property of the ion channel is its conductivity. The conductance of ion channels may range from few pS up to hundreds pS, depending on the it's kinetic properties [1].

Nanoparticles (NPs) are polymeric particle systems with sizes in the range of 1–100 nm, prepared with natural or synthetic polymers. The physical and chemical properties of NPs are determined by their small size and surface area [2]. Nowadays, NP technology is widely used in industry, biochemistry, cosmetics, environmental engineering, optics, electronics, telecommunications, pharmacology, medicine, food and cosmetics [3]. The small size of NPs allows them to pass through the epithelial and endothelial barriers into lymph and blood and be transported through the bloodstream and lymph flow to the liver, heart, brain, spleen, nervous system and bone marrow. In addition, they can enter cells by transcytosis mechanisms or by diffusion across the cell membrane [4]. In recent years, many studies have reported that nanoparticles can interact with ion channels and alter their currents, channel kinetics, subcellular localization, and expression levels of proteins related to the ion channel [5–9]. SiO_2 nanoparticles are one of the most widely used nanoparticles in medical imaging, drug delivery systems, cancer treatment and biosensor technology due to their physicochemical properties [10]. SiO_2 nanoparticles have the property of evaporation easily in air due to their very low density [11]. They are easily inhaled and enter the organism and cause pulmonary and cardiovascular changes such as pulmonary inflammation, myocardial ischemic damage, atrio-ventricular blockade, increase in blood fibrinogen concentration and blood viscosity [12]. In addition, SiO_2 NPs cause DNA damage in

* Corresponding author.
E-mail address: ucomelek@yahoo.com (Ü. Çömelekoglu).

https://doi.org/10.1016/j.mehy.2023.111081
Received 17 November 2022; Received in revised form 13 March 2023; Accepted 9 April 2023
Available online 21 April 2023

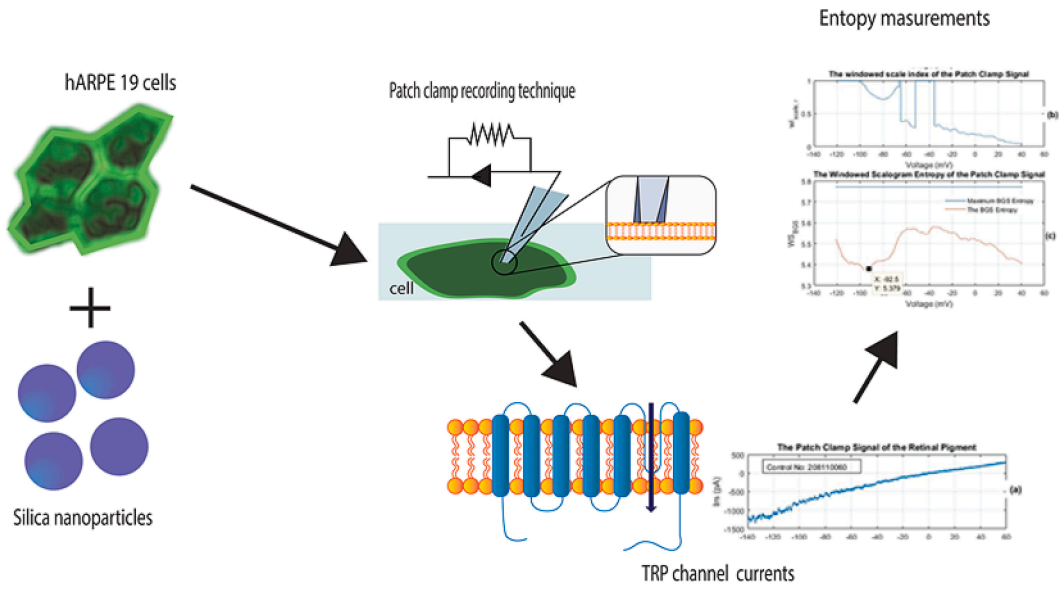

Fig. 1. The schematic diagram of the hypothesis evaluation.

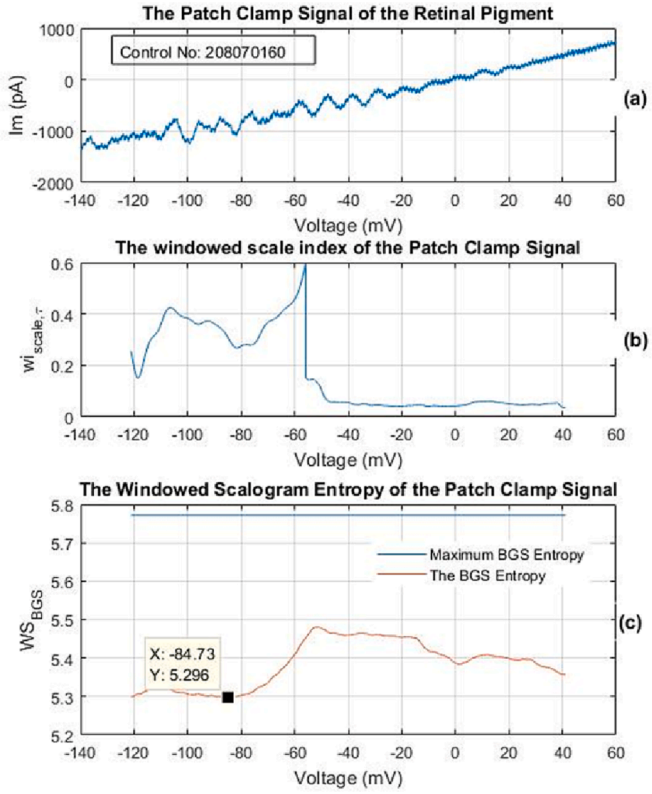

Fig. 2. The WndSI and WndSE for the patch clamp signal of the retinal pigment epithelium cell with registration number 208070160 in the control group. The windowed scalograms of the patch clamp signal were calculated for the time radius $\tau = 600$ time steps and the 'Morlet wavelet function' in the scale range $[s_0 = 8, s_1 = 256]$. **(a)** The patch clamp signal of a retinal pigment epithelium cell obtained by increasing the potential from −140 mV to +60 mV as temporal, for the control measurement **(b)** The WndSI spectrum indicates the temporal evolution of the non-periodicity degree of the patch clamp signal. **(c)** The WndSE spectrum indicates the temporal evolution of the BGS entropy of the patch clamp signal.

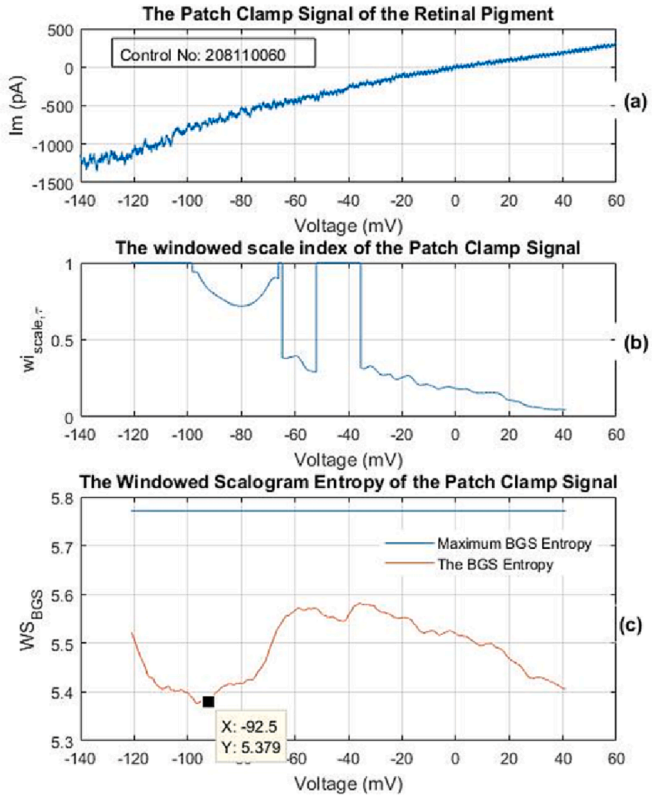

Fig. 3. The WndSI and WndSE for the patch clamp signal of the retinal pigment epithelium cell with registration number 208110060 in the control group. The windowed scalograms of the patch clamp signal were calculated for the time radius $\tau = 600$ time steps and the 'Morlet wavelet function' in the scale range $[s_0 = 8, s_1 = 256]$. **(a)** The patch clamp signal of a retinal pigment epithelium cell obtained by increasing the potential from −140 mV to +60 mV as temporal, for the control measurement **(b)** The WndSI spectrum indicates the temporal evolution of the non-periodicity degree of the patch clamp signal. **(c)** The WndSE spectrum indicates the temporal evolution of the BGS entropy of the patch clamp signal.

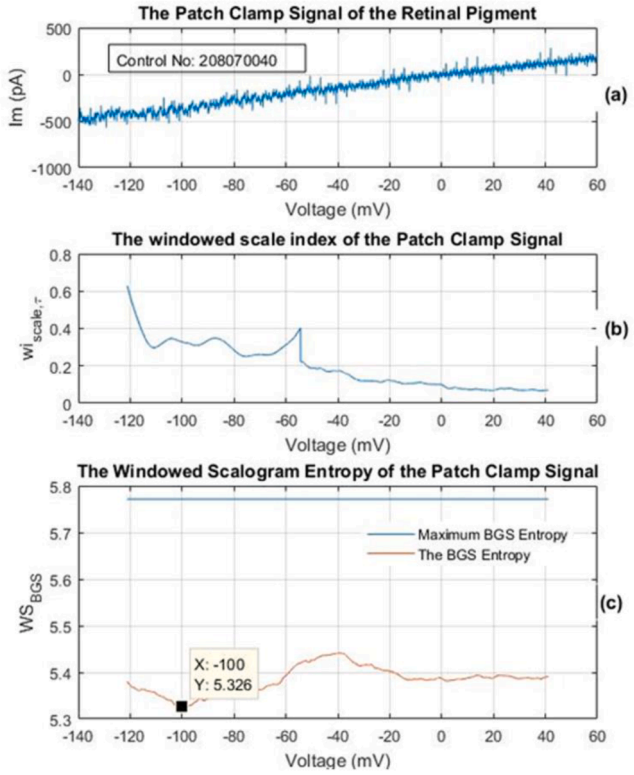

Fig. 4. The WndSI and WndSE for the patch clamp signal of the retinal pigment epithelium cell with registration number 208070040 in the control group. The windowed scalograms of the patch clamp signal were calculated for the time radius $\tau = 600$ time steps and the 'Morlet wavelet function' in the scale range $[s_0 = 8, s_1 = 256]$. **(a)** The patch clamp signal of a retinal pigment epithelium cell obtained by increasing the potential from −140 mV to +60 mV as temporal, for the control measurement **(b)** The WndSI spectrum indicates the temporal evolution of the non-periodicity degree of the patch clamp signal. **(c)** The WndSE spectrum indicates the temporal evolution of the BGS entropy of the patch clamp signal.

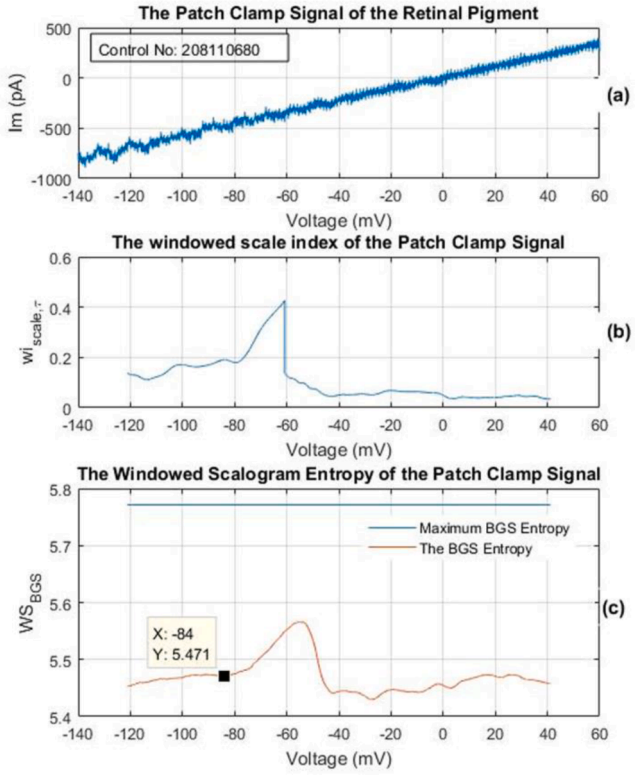

Fig. 5. The WndSI and WndSE for the patch clamp signal of the retinal pigment epithelium cell with registration number 208110680 in the control group. The windowed scalograms of the patch clamp signal were calculated for the time radius $\tau = 600$ time steps and the 'Morlet wavelet function' in the scale range $[s_0 = 8, s_1 = 256]$. **(a)** The patch clamp signal of a retinal pigment epithelium cell obtained by increasing the potential from −140 mV to +60 mV as temporal, for the control measurement **(b)** The WndSI spectrum indicates the temporal evolution of the non-periodicity degree of the patch clamp signal. **(c)** The WndSE spectrum indicates the temporal evolution of the BGS entropy of the patch clamp signal.

human lymphocytes [13], and may cause changes in the electrical and mechanical activity of the heart [14]. It has been shown that amorphous SiO_2 NPs cause inflammation in the lungs and cause apoptosis and cell death through reactive oxygen species [15]. The effects of nanoparticles on cells may be influenced by various properties, including the nanomaterial's size, shape, surface properties and surface area. There are many methods to reduce the toxic effects of nanoparticles. Studies have shown that changing the shape and size of particles, and methods to modify their surface, can lead to the the production of nanoparticles with lower toxicity [16].

The retinal pigment epithelium (RPE) consists of a single layer of regular polygonal cells arranged in the outermost layer of the retina. The RPE cytoskeleton is highly associated with its distinct functions such as melanosome transport and phagocytosis. The cytoskeleton is composed of three major elements: the actin microfilaments, microtubules, and intermediate filaments. They play an important role in the generation and maintenance of cellular shape and cell migration. The lateral membranes of RPE cells are joined by a continuous belt of tight junctions which form the outer blood-retinal barrier. Cells contain a basal nucleus and plenty of organelles which reflect the high metabolic rate of the RPE [17,18]. The outer side of the RPE is attached to Bruch's membrane and the choroid, and the inner side to the outer segment of photoreceptor cells [19]. These cells have many important functions as the synthesis and transport of substances necessary for the normal functioning of photoreceptors [20], the production of melanin pigment for the absorption of light and the phagocytosis of the photoreceptor outer segments [21], the release of cytokines and growth factors [22] and regulation of the local immune response in the eye [23]. The retinal pigment epithelium has an important role in the maintenance of visual function. Many retinal diseases are associated with changes in the RPE [19].

A number of cellular functions of RPE are controlled by intracellular calcium. Intracellular free Ca^{2+} concentration is necessary for the continue of normal retinal function [24]. In the RPE, L-type calcium channels and purinergic receptor channels open only in response to depolarization or binding of ATP. Calcium is removed from the cell via active plasma membrane Ca2+ ATPases and Na^{+}/Ca^{2+} exchangers. Thus, unstimulated RPE cells stabilizes intracellular calcium of about 80–100 nM. It is known that transient receptor (TRP) channel currents play an important role in this stabilization in the RPE cells [24].

Entropy measures plays important roles in analyzing the temporal statistical nature of dynamical systems evolving in time such as biological, physiological, physical, econometric, and social. In an information-theoretic framework, the information of dynamical systems varies at each time step. Entropy is defined as a measure of probability of microstates being in different energy states in a system [25,26]. The behavior of the cells can be analyzed by observing temporal evolution of entropy in the time series obtained from the measurable processes of cells. The distribution of ionic currents in cells varies when different electrical potential are applied. Depending on the electrical potential change, the entropy values also change.

In this study for the first time, we used windowed scalogram entropy

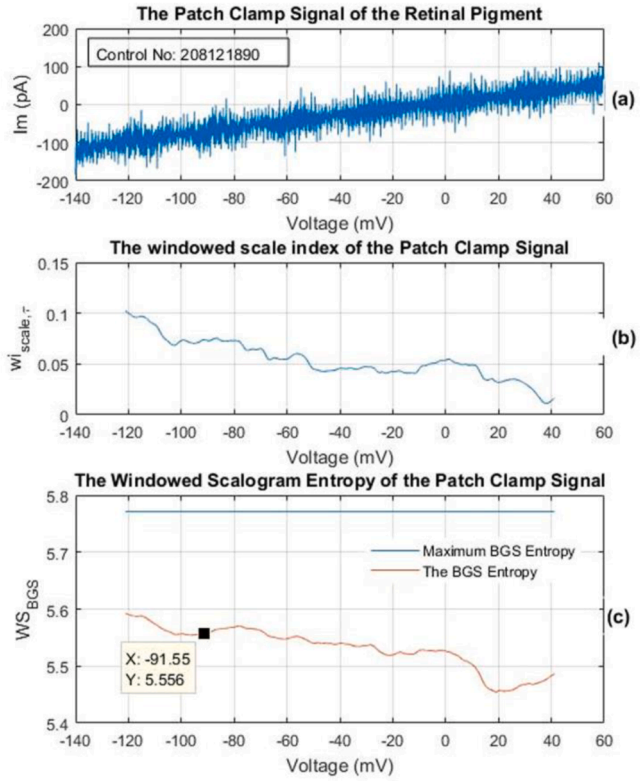

Fig. 6. The WndSI and WndSE for the patch clamp signal of the retinal pigment epithelium cell with registration number 208121890 in the control group. The windowed scalograms of the patch clamp signal were calculated for the time radius $\tau = 600$ time steps and the 'Morlet wavelet function' in the scale range $[s_0 = 8, s_1 = 256]$. **(a)** The patch clamp signal of a retinal pigment epithelium cell obtained by increasing the potential from −140 mV to +60 mV as temporal, for the control measurement **(b)** The WndSI spectrum indicates the temporal evolution of the non-periodicity degree of the patch clamp signal. **(c)** The WndSE spectrum indicates the temporal evolution of the BGS entropy of the patch clamp signal.

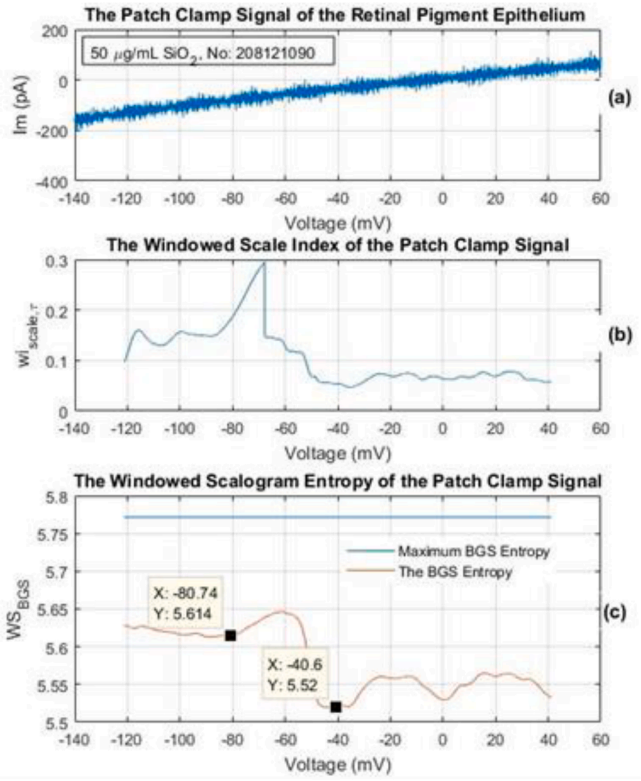

Fig. 7. The WndSI and WndSE for the patch clamp signal of the retinal pigment epithelium cell with registration number 208121090 in the 50 μM SiO_2 group. The windowed scalograms of the patch clamp signal were calculated for the time radius $\tau = 600$ time steps and the 'Morlet wavelet function' in the scale range $[s_0 = 8, s_1 = 256]$. **(a)** The patch clamp signal of a retinal pigment epithelium cell obtained by increasing the potential from −140 mV to +60 mV as temporal, for the SiO_2 dose of 50 μM **(b)** The WndSI spectrum indicates the temporal evolution of the non-periodicity degree of the patch clamp signal. **(c)** The WndSE spectrum indicates the temporal evolution of the BGS entropy of the patch clamp signal.

to quantify the temporal entropy changes of TRP currents in RPE cells exposed to SiO_2 nanoparticles, and compare the results with windowed scale index method. We used MATLAB program (MATLAB R2017a, 1994–2023 The MathWorks, Inc. USA) in all calculations and graphic drawings.

The hypothesis

Nanoparticles are very small-sized material with dimensions ranging from 1 to 100 nm. This particles are widely used in different areas in industry and medicine. They can enter to body through different routes including the inhalation, skin, intravenous injections and ingestio and interact cell membranes and ion channels in the membrane. The functions of ion channels can be investigated with the patch clamp technique. This technique is used to detect the ionic currents of ion channels. The analysis of ionic currents gives information about the current–voltage relationship, relative density, activation and inactivation kinetics of ion channels. In this study, we hypothesize that we can analyze ion channel currents with the windowed scalogram entropy method, unlike the methods used so far. To test our hypothesis, we chose silica nanoparticle - transient receptor potential channels interaction in retinal pigment epithelium cells. In addition, we hypothesized that this method could be used to reveal all other nanoparticle-ion channel interactions.

Evaluation of the hypothesis

SiO_2 nanoparticles

Commercially purchased SiO_2 nanoparticles (Sigma Aldrich, catalog no: 637246, S Louis, MO, USA) were 99.5% pure and powdered according to the manufacturer's catalog information and had a surface area of 590–690 m^2/g. The size of the particles was in the range of 5–15 nm.

Cell culture

In this study, ARPE-19 human retinal pigment culture cells were used (ATCC CRL-2302; American Type Culture Collection (ATCC), Manassas, VA, USA). The cell line was purchased commercially. Therefore, ethics committee approval was not required for the study. The cells were kept frozen in liquid nitrogen until use. Incubation environments are 37 °C under humid atmosphere and 5% CO_2 pressure. Dulbecco's modified Eagle's medium (DMEM F12) supplemented with 10% fetal bovine serum (FBS), 2 mM GlutaMAX, 1% Penicillin-streptomycin, 1% amphotericin was used for growth media. The prepared medium with additive was stored at +4 °C. 4–6 h after seeding, the growth medium of the cells was replaced with fresh supplemented medium. The medium were changed every three days. After approximately 7 days, 80% confluent cells were passaged until they reached the required number in experiments.

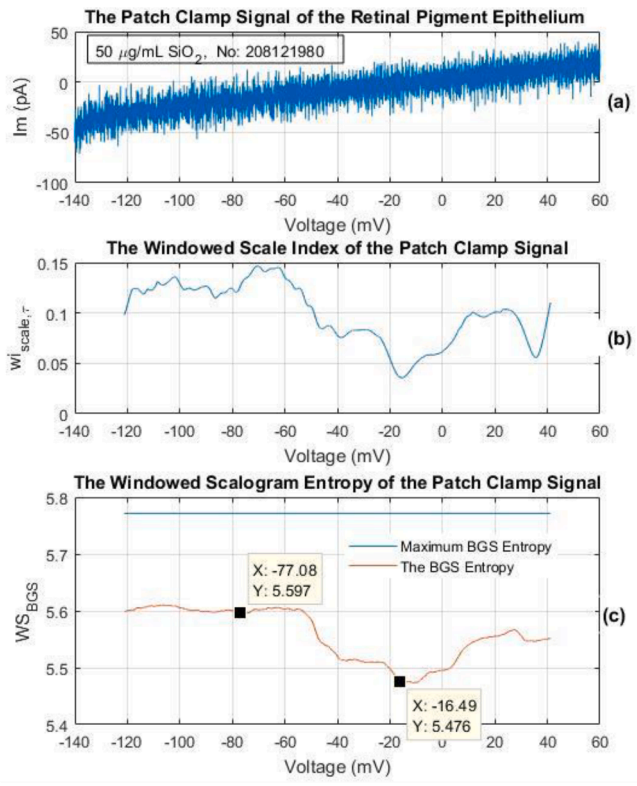

Fig. 8. The WndSI and WndSE for the patch clamp signal of the retinal pigment epithelium cell with registration number 208121980 in the 50 μM SiO_2 group. The windowed scalograms of the patch clamp signal were calculated for the time radius $\tau = 600$ time steps and the 'Morlet wavelet function' in the scale range $[s_0 = 8, s_1 = 256]$. **(a)** The patch clamp signal of a retinal pigment epithelium cell obtained by increasing the potential from −140 mV to +60 mV as temporal, for the SiO_2 dose of 50 μM **(b)** The WndSI spectrum indicates the temporal evolution of the non-periodicity degree of the patch clamp signal. **(c)** The WndSE spectrum indicates the temporal evolution of the BGS entropy of the patch clamp signal.

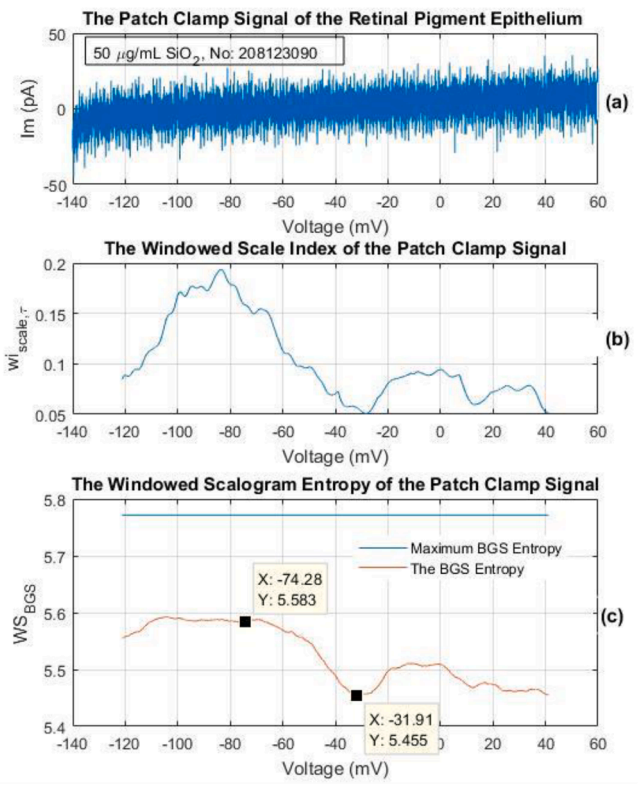

Fig. 9. The WndSI and WndSE for the patch clamp signal of the retinal pigment epithelium cell with registration number 208123090 in the 50 μM SiO_2 group. The windowed scalograms of the patch clamp signal were calculated for the time radius $\tau = 600$ time steps and the 'Morlet wavelet function' in the scale range $[s_0 = 8, s_1 = 256]$. **(a)** The patch clamp signal of a retinal pigment epithelium cell obtained by increasing the potential from −140 mV to +60 mV as temporal, for the SiO_2 dose of 50 μM **(b)** The WndSI spectrum indicates the temporal evolution of the non-periodicity degree of the patch clamp signal. **(c)** The WndSE spectrum indicates the temporal evolution of the BGS entropy of the patch clamp signal.

Determination of SiO_2 nanoparticle concentrations

Real-time cell analysis system (xCELLigence, ACEA Biosciences, San Diego, CA, USA) was used to determine the SiO_2 concentrations to be used in the study. With the xCELLigence system, cellular events can be analyzed in real time. The system measures electrical impedance using micro-electrodes placed in the e-plates 16. Impedance measurement inform quantitative information about the biological state of cells such as viability [27]. The xCELLigence system was used in accordance with the manufacturer's instructions.

Selection of treatment concentrations and experimental design

In the present study, to determine the treatment concentration of SiO_2 nanoparticles, ARPE 19 cells were treated with 1, 5, 10, 25, 50, 100 and 150 μg/mL SiO_2 NPs and for each concentration, the cell index value was calculated with the The xCELLigence system. The three concentrations with the lowest cell index values (50, 100 and 150 μg/mL) were selected to test the hypothesis of this study. These selected concentrations are also compatible with the doses in studies investigating the cytotoxic effect of SiO_2 nanoparticles on different cells [28–30].

Patch- clamp recordings

The whole-cell mode of the patch-clamp method was used for electrobiophysical analysis [17]. Measurements were made for control, 50, 100 and 150 μg/mL SiO_2 NP groups. Bath solution content (mM) was 130 NaCl, 5 CsCl, 2 $MgCl_2$, 2 $CaCl_2$, 10 HEPES and 5 glucose (pH 7.3 with CsOH) Pipette solution (mM) was prepared to contain 140 CsCl, 2 $MgCl_2$, 1 $CaCl_2$, 2.5 EGTA and 10 HEPES, (pH adjusted to 7.3 with CsOH). Two-channel computer-controlled Multi-Clamp 700B (Axon Instruments, CA, USA) amplifier and Digidata 1322A (Axon Instruments, USA) digital converter were used in the recordings. BM-37XB (U-Therm International (H. K.) Limited) invert microscope was used to monitor the cell and pipette during recordings. Measurements were recorded by Clampex 9.2 (Axon Instruments, USA) software. Clamping resistance was evaluated by recording current with the protocol application to the cell membrane, and analyzed with Clamp fit 10 (Axon Instruments, CA, USA) software. After obtaining a sealing resistance of 1–10 GΩ between the cell and the pipette, the membrane potential was clamped to −40 mV. A ramp of 1000 ms duration was used for stimulation [31]. The ramp was increased from −140 mV to +60 mV [32]. Data were analyzed with Clampfit 10 software (Axon Instruments, CA, USA). The peak value of TRP currents were measured at +60 mV voltage value in all groups. The experiment was performed at room temperature (24–25 °C).

The Boltzmann-Gibbs-Shannon (BGS) entropy

As is known, entropy is defined differently in different contexts. Firstly, entropy (S) which is the second law of thermodynamics refers to the energy that cannot be converted into work. Also, disorders in systems are measured by entropy. Secondly, entropy is used in the sense of

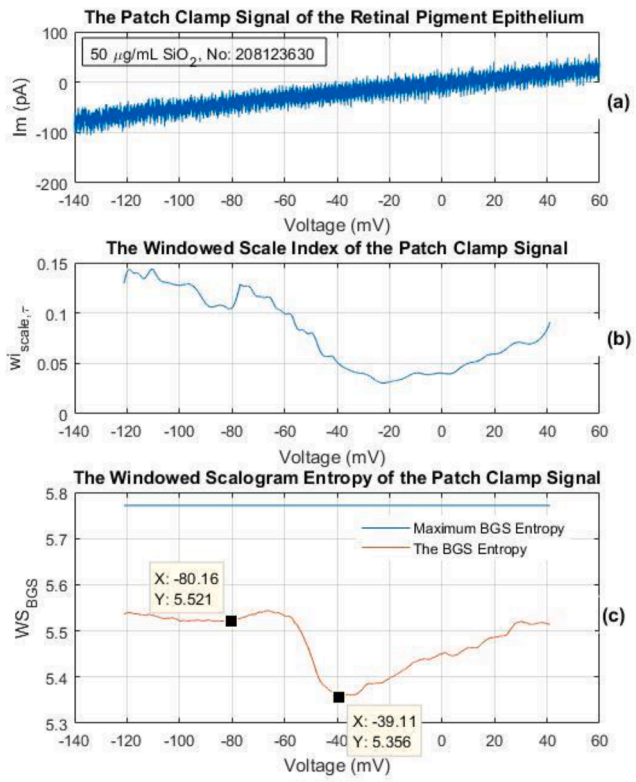

Fig. 10. The WndSI and WndSE for the patch clamp signal of the retinal pigment epithelium cell with registration number 208123630 in the 50 μM SiO_2 group. The windowed scalograms of the patch clamp signal were calculated for the time radius $\tau = 600$ time steps and the 'Morlet wavelet function' in the scale range [$s_0 = 8, s_1 = 256$]. **(a)** The patch clamp signal of a retinal pigment epithelium cell obtained by increasing the potential from −140 mV to +60 mV as temporal, for the SiO_2 dose of 50 μM **(b)** The WndSI spectrum indicates the temporal evolution of the non-periodicity degree of the patch clamp signal. **(c)** The WndSE spectrum indicates the temporal evolution of the BGS entropy of the patch clamp signal.

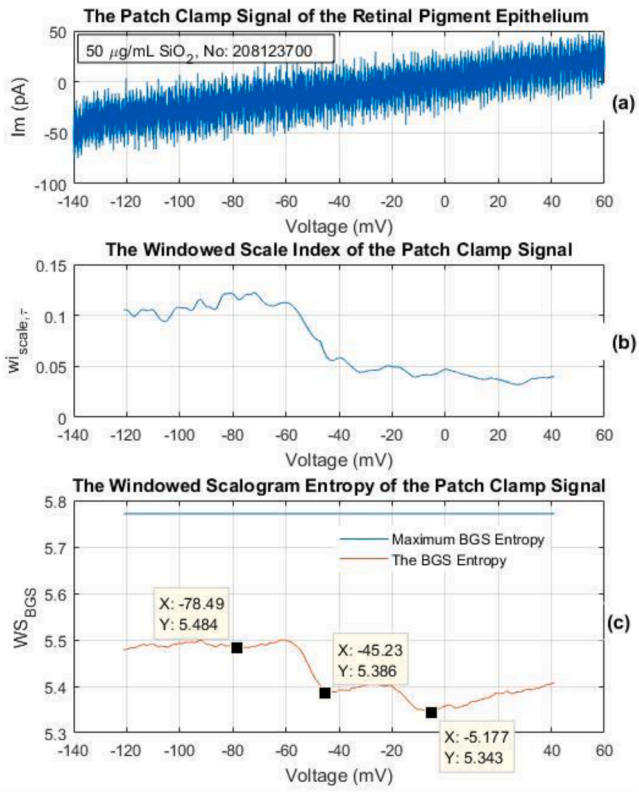

Fig. 11. The WndSI and WndSE for the patch clamp signal of the retinal pigment epithelium cell with registration number 208123700 in the 50 μM SiO_2 group. The windowed scalograms of the patch clamp signal were calculated for the time radius $\tau = 600$ time steps and the 'Morlet wavelet function' in the scale range [$s_0 = 8, s_1 = 256$]. **(a)** The patch clamp signal of a retinal pigment epithelium cell obtained by increasing the potential from −140 mV to +60 mV as temporal, for the SiO_2 dose of 50 μM **(b)** The WndSI spectrum indicates the temporal evolution of the non-periodicity degree of the patch clamp signal. **(c)** The WndSE spectrum indicates the temporal evolution of the BGS entropy of the patch clamp signal.

information theory or uncertainty [33–36].

Clausius inequality describes the change in total entropy of a system, $\Delta S \geq \Delta Q/T$. Where ΔQ is heat transfer, T is temperature. Boltzmann showed that entropy is related to the probabilistic state. The Boltzmann-Gibbs-Shannon (BGS) entropy can be written as follows for discrete random variables

$$S_{BGS}(p) = -k\sum_{i=1}^{w} p_i ln p_i \tag{1}$$

Here, W indicates the number of microscopic states of the system and p_i is i th state probability of the system. k, a positive constant, represents the unit of entropy measurement. The value of Boltzmann's constant in thermodynamics is $k_B = 1.3810^{-23}\frac{J}{K}$. In Information theory, the value of k is one. If $p_i = \frac{1}{W}$, BGS entropy (1) reaches its maximum value;

$$S_{BGS_{max}} = kln(W) \tag{2}$$

Here, Boltzmann's equation (2) states that the probability of microstates in thermodynamic equilibrium is equal.

Basic concepts of wavelet transform

Wavelet analysis is a mathematical approach widely used for non-stationary signal processing applications. It reveals the frequency components of signals in the temporal or spatial domain. A wavelet is formulated as below [37,38]

$$\int_{-\infty}^{+\infty} \psi(t)dt = 0, \psi \in L^2(R), \tag{3}$$

normalized $\|\psi\| = 1$, and built around $t = 0$. The wavelet function ψ can be written as below;

$$\psi_{j,k}(t) = \frac{1}{\sqrt{2^j}}\psi\left(\frac{t-2^j k}{2^j}\right) \tag{4}$$

where $j, k \in Z$. s defines the scale and and u defines the shift of time.

$$\psi_{u,s}(t) = \frac{1}{\sqrt{s}}\psi\left(\frac{t-u}{s}\right), \quad u \in R, s > 0 \tag{5}$$

Which remains normalized: $\|\psi_{u,s}\| = 1$. For a signal $f(t) \in L^2(R)$, the continuous wavelet transform (CWT) is defined as follows;

$$Wf(u,s) = \langle f, \psi_{u,s} \rangle = \int_{-\infty}^{+\infty} f(t)\psi_{u,s}^{*}(t)dt \tag{6}$$

The scalogram $S(s)$ of $f(t)$ that is the energy of the CWT is defined as;

$$S(s) = \|Wf(u,s)\| = \left(\int_{-\infty}^{+\infty} |Wf(u,s)|^2 du\right)^{1/2} \tag{7}$$

The scalogram of $f(t)$ at scale s calculates the energy of $f(t)$. That is, the scalogram (7) gives the energy values of $f(t)$ plotted as a function of

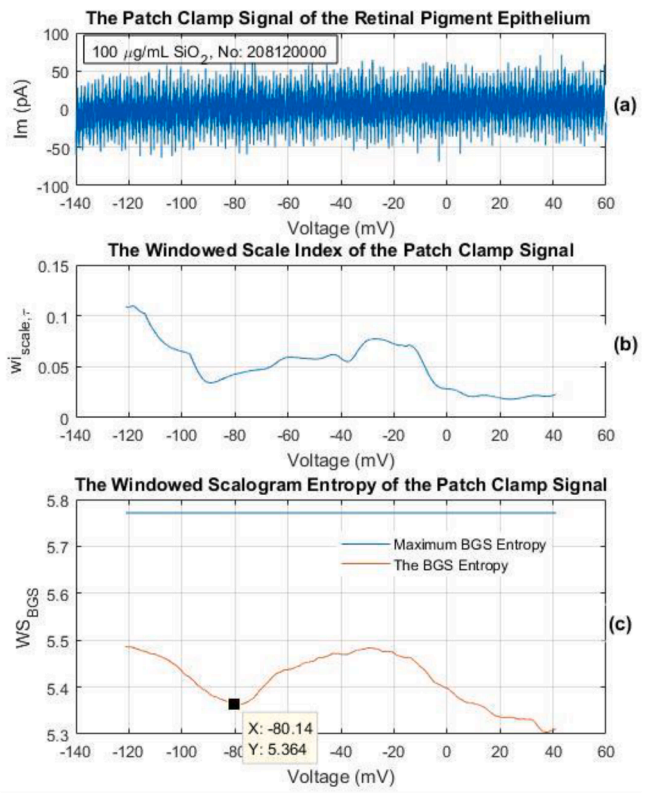

Fig. 12. The WndSI and WndSE for the patch clamp signal of the retinal pigment epithelium cell with registration number 208120000 in the 100 μM SiO_2 group. The windowed scalograms of the patch clamp signal were calculated for the time radius $\tau = 600$ time steps and the 'Morlet wavelet function' in the scale range $[s_0 = 8, s_1 = 256]$. **(a)** The patch clamp signal of a retinal pigment epithelium cell obtained by increasing the potential from −140 mV to +60 mV as temporal, for the SiO_2 dose of 100 μM **(b)** The WndSI spectrum indicates the temporal evolution of the non-periodicity degree of the patch clamp signal. **(c)** The WndSE spectrum indicates the temporal evolution of the BGS entropy of the patch clamp signal.

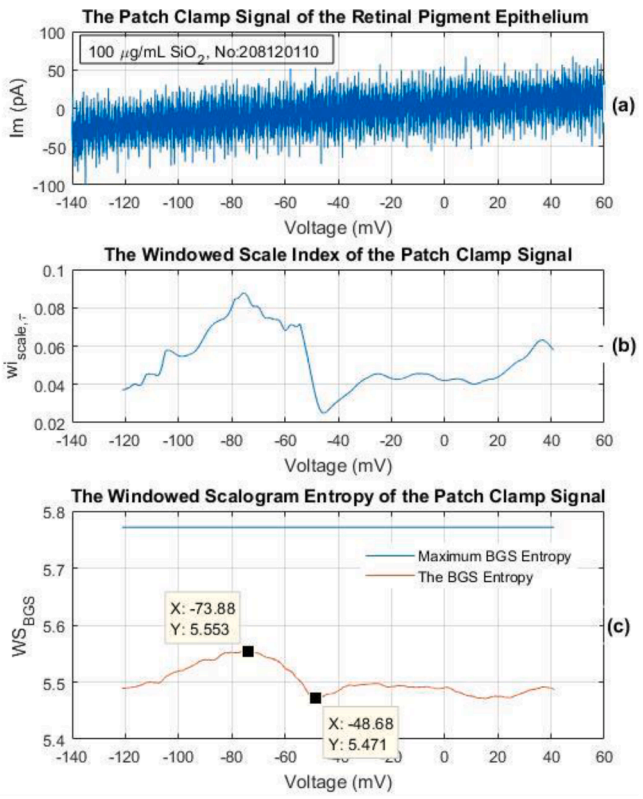

Fig. 13. The WndSI and WndSE for the patch clamp signal of the retinal pigment epithelium cell with registration number 208120110 in the 100 μM SiO_2 group. The windowed scalograms of the patch clamp signal were calculated for the time radius $\tau = 600$ time steps and the 'Morlet wavelet function' in the scale range $[s_0 = 8, s_1 = 256]$. **(a)** The patch clamp signal of a retinal pigment epithelium cell obtained by increasing the potential from −140 mV to +60 mV as temporal, for the SiO_2 dose of 100 μM **(b)** The WndSI spectrum indicates the temporal evolution of the non-periodicity degree of the patch clamp signal. **(c)** The WndSE spectrum indicates the temporal evolution of the BGS entropy of the patch clamp signal.

time and frequency.

Windowed scalogram entropy (WndSE)

Physiological systems that generates biological signals are the nonlinear dynamical processes. Naturally, entropy changes significantly over time for dynamic processes. For these cases, windowed scalogram entropy (WndSE) is a method that can be calculated the temporal change of entropy of a time series. This method based on the windowed scalogram [39].

Using equation (7), the windowed scalogram of a time series f is defined as in equation (8) [40,41].

$$WS_\tau(t,s) = \left(\int_{t-\tau}^{t+\tau} |Wf(u,s)|^2 du \right)^{1/2} \tag{8}$$

Here,t is the time vector centering the windows and τ is the time radius of the windows. s is the vector of the scales. The windowed scalogram (8) is the scalogram (7) limited to a short time interval $[t-\tau, t+\tau]$. The windowed scalograms are normalized within specified scales for each time window. Thus, discrete solutions of the $WS_\tau(t,s)$ in equation (8) give energies at all scales corresponding to the frequency components for each time window of a time series.

The probability distributions of the energies of the normalized windowed scalograms for each time window can be given as in equation (9)

$$P_{s,\tau}(t) = \frac{WS_\tau(t,s)}{\sum_{s_0}^{s_1} WS_\tau(t,s)} \tag{9}$$

where, $\sum_{s_0}^{s_1} WS_\tau(t,s)$ is the total energy of the time window, $WS_\tau(t,s)$ is energy at s scale. The sum of the probabilities at each scale of the time window is equal to one.

$$\sum_{s_0}^{s_1} P_{s,\tau}(t) = 1 \tag{10}$$

From equation (1) and equation (9), the BGS entropy for time windows can be rewritten as in equation (11).

$$WS(P) \equiv -k \sum_{s_0}^{s_1} P_{s,\tau}(t) ln P_{s,\tau}(t) \tag{11}$$

The temporal change of entropy of biological signals can be measured by "windowed scalogram entropy" (11).

Windowed scale index (WndSI)

The windowed scale index (WndSI) measures the degree of the aperiodicity of the signal over time. The WndSI of periodic signals is close to zero [39–28].

For a time series with time radius τ, centered at time t, in the scale

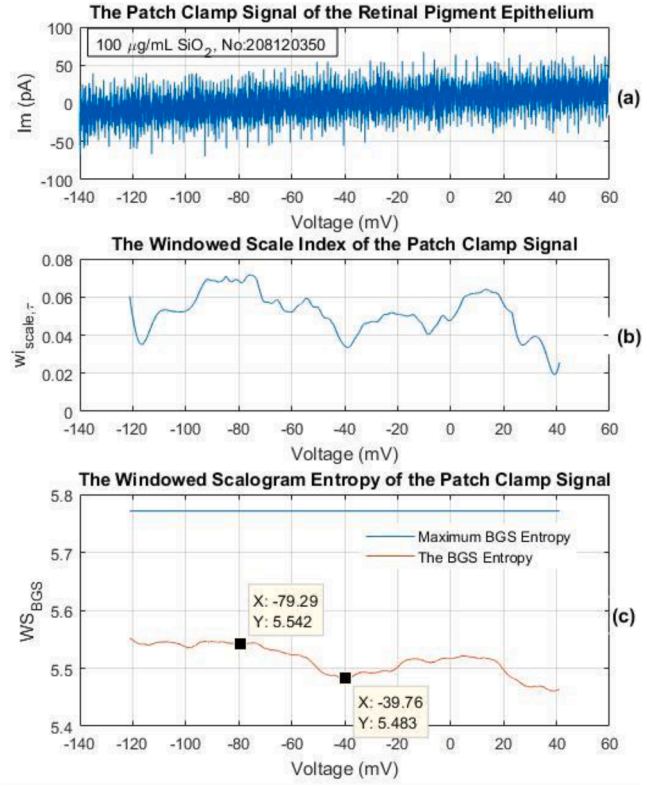

Fig. 14. The WndSI and WndSE for the patch clamp signal of the retinal pigment epithelium cell with registration number 208120350 in the 100 μM SiO_2 group. The windowed scalograms of the patch clamp signal were calculated for the time radius $\tau = 600$ time steps and the 'Morlet wavelet function' in the scale range $[s_0 = 8, s_1 = 256]$. **(a)** The patch clamp signal of a retinal pigment epithelium cell obtained by increasing the potential from −140 mV to +60 mV as temporal, for the SiO_2 dose of 100 μM **(b)** The WndSI spectrum indicates the temporal evolution of the non-periodicity degree of the patch clamp signal. **(c)** The WndSE spectrum indicates the temporal evolution of the BGS entropy of the patch clamp signal.

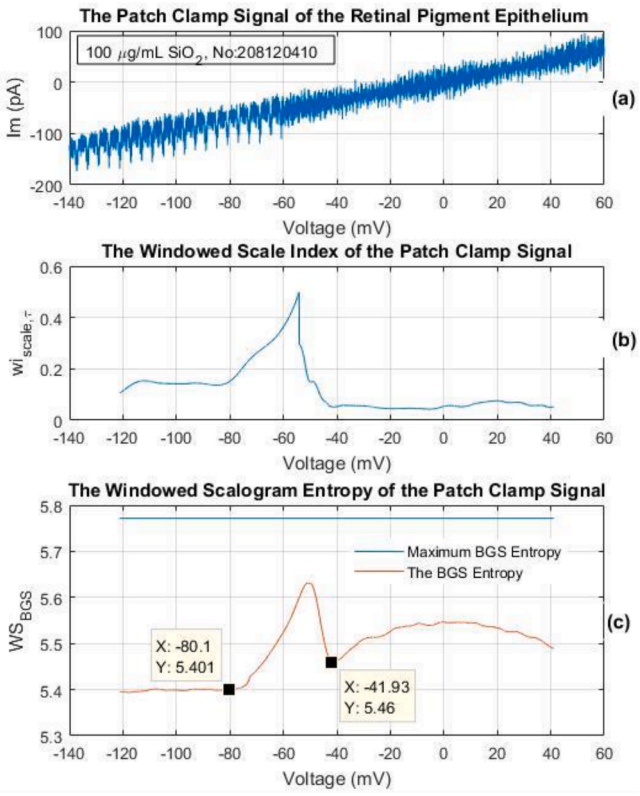

Fig. 15. The WndSI and WndSE for the patch clamp signal of the retinal pigment epithelium cell with registration number 208120410 in the 100 μM SiO_2 group. The windowed scalograms of the patch clamp signal were calculated for the time radius $\tau = 600$ time steps and the 'Morlet wavelet function' in the scale range $[s_0 = 8, s_1 = 256]$. **(a)** The patch clamp signal of a retinal pigment epithelium cell obtained by increasing the potential from −140 mV to +60 mV as temporal, for the SiO_2 dose of 100 μM **(b)** The WndSI spectrum indicates the temporal evolution of the non-periodicity degree of the patch clamp signal. **(c)** The WndSE spectrum indicates the temporal evolution of the BGS entropy of the patch clamp signal.

interval $[s_0, s_1]$, the WndSI is defined as in equation (12) [38–28].

$$wi_{scale,\tau}(t) = \frac{WS_\tau(t, s_{min})}{WS_\tau(t, s_{max})} \tag{12}$$

Here, s_{max} is the lowest scale such that $WS_\tau(t, s) \leq WS_\tau(t, s_{max})$ for all $s \in [s_0, s_1]$, and s_{min} is the lowest scale such that $WS_\tau(t, s_{min}) \leq WS_\tau(t, s)$ for all $s \in [s_{max}, 2s_1]$.

Fig. 1 shows the schematic representation of the hypothesis evaluation.

Statistical analysis

The results were statistically analyzed using "SPSS (ver.23. Armonk, NY: IBM Corp)". To check normality of variables, "Shapiro Wilk test" was used. One-way ANOVA test was used for differences between groups, and the Fisher's Least Significant Difference Test (LSD) was used for multiple comparisons. Data were expressed as "Mean ± Standard Error". Statistical significance levels were considered as $p < 0.05$.

Results

Entropy measurement

For entropy measurement, we used the time series of the ionic currents recorded from retinal pigment epithelium cells by the whole-cell patch-clamp technique. The WndSE and WndSI are calculated from the windowed scalogram (8). The WndSE (11) and WndSI (12) were computed for the patch-clamp signals of the retinal pigment epithelium cells. Here, we worked out the windowed scalograms of the patch-clamp signals using the time radius $\tau = 600$ time steps for 'Morlet wavelet function' with the scales between $s_0 = 8$ and $s_1 = 256$.

Figs. 2–6 show graphs that are the patch clamp signals of the retinal pigment epithelium cells, the WndSI and WndSE for control group. Figs. 7–19 show graphs plotted for the SiO_2 doses of 50 μg/mL (7-11), 100 μg/mL (12-15) and 150 μg/mL (16-19) respectively.

To evaluate the results of the graphs in Figs. 2(c)–19(c); the mean and standard deviation (sd.) values of the windowed scalogram (WS) entropies and the values of the WS entropies at certain voltages are given in Table 1. Also, Table 2 shows the general summary of the WS entropy values (of Table 1).

For voltage values less than −40 mV, Figs. 2(c)–19(c) and Table 1 and 2 show that the WS entropy values of RPE cells exposed to SiO2 nanoparticles increase compared to the control group. These results can be written as an inequality that $(WS)_{controlRPE} < (WS)_{SiO_2-RPE}$ for $Voltaj < -40mV$. For voltage values greater than −40 mV, there is no significant difference between RPE cell entropies.

On the other hand, when Figures are analyzed from another perspective; at applied potentials in the range of −140 to +60 mV, the mean voltage value at which the entropy of retinal pigment epithelial cells is minimal for the control group is −90.55 ± 2.92 mV. This values are −26.65 ± 6.86 mV in the 50 μg/mL SiO_2 NP group, −43.44 ± 2.67 mV in the 100 μg/mL SiO_2 NP group, and −10.92 ± 8.36 mV in the 150

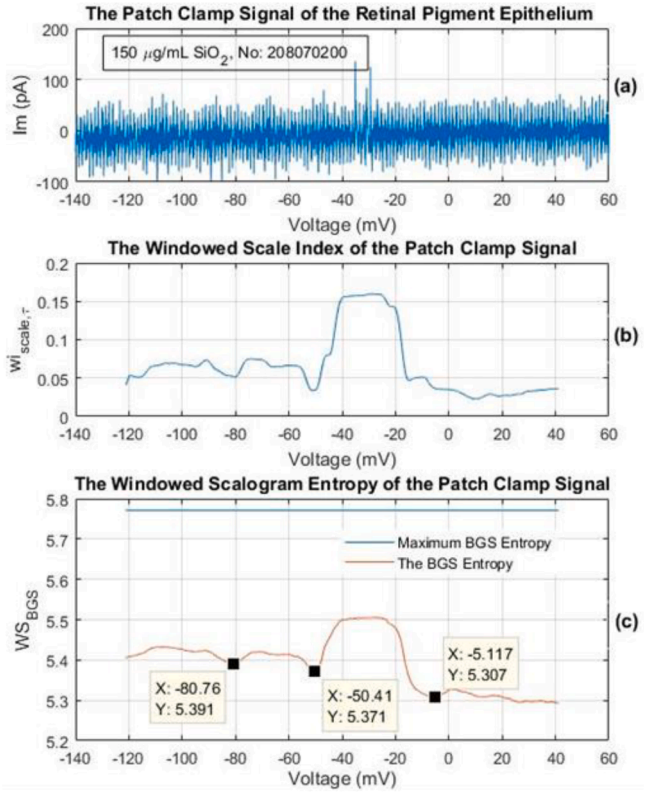

Fig. 16. The WndSI and WndSE for the patch clamp signal of the retinal pigment epithelium cell with registration number 208070200 in the 150 μM SiO_2 group. The windowed scalograms of the patch clamp signal were calculated for the time radius $\tau = 600$ time steps and the 'Morlet wavelet function' in the scale range $[s_0 = 8, s_1 = 256]$. **(a)** The patch clamp signal of a retinal pigment epithelium cell obtained by increasing the potential from −140 mV to +60 mV as temporal, for the SiO_2 dose of 150 μM **(b)** The WndSI spectrum indicates the temporal evolution of the non-periodicity degree of the patch clamp signal. **(c)** The WndSE spectrum indicates the temporal evolution of the BGS entropy of the patch clamp signal.

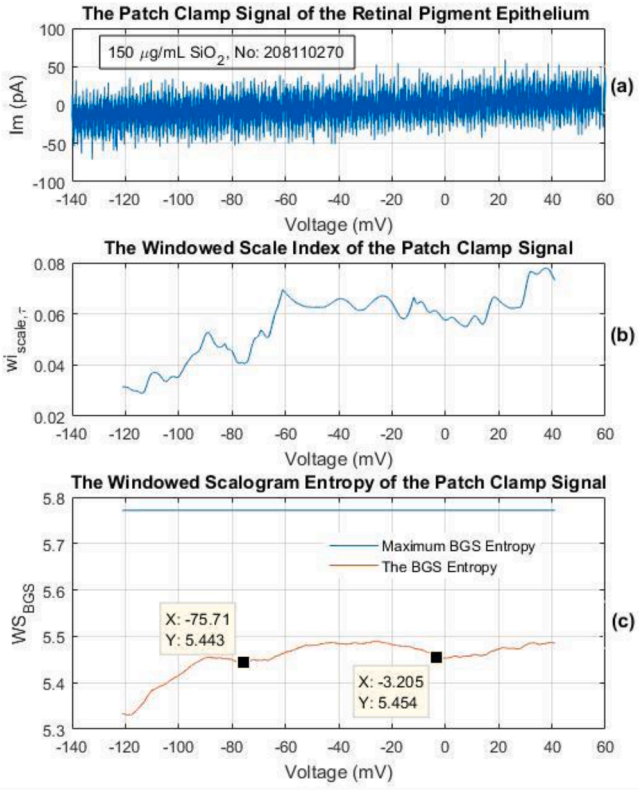

Fig. 17. The WndSI and WndSE for the patch clamp signal of the retinal pigment epithelium cell with registration number 208110270 in the 150 μM SiO_2 group. The windowed scalograms of the patch clamp signal were calculated for the time radius $\tau = 600$ time steps and the 'Morlet wavelet function' in the scale range $[s_0 = 8, s_1 = 256]$. **(a)** The patch clamp signal of a retinal pigment epithelium cell obtained by increasing the potential from −140 mV to +60 mV as temporal, for the SiO_2 dose of 150 μM **(b)** The WndSI spectrum indicates the temporal evolution of the non-periodicity degree of the patch clamp signal. **(c)** The WndSE spectrum indicates the temporal evolution of the BGS entropy of the patch clamp signal.

μg/mL SiO_2 NP group. Voltage values at which minimum entropy were significantly increased in all dose groups compared to control group. ($p < 0.05$). The difference between dose groups was also significant ($p < 0.05$).

Consequences of the hypothesis and discussion

In this study, whole-cell patch clamp technique was used to record the TRP channel currents in RPE cells. To analyze these currents, we used nonlinear analysis methods and obtained entropy values. This study is important as it is the first to analyze nanoparticle-ion channel interaction using the entropy measure.

The cell is a complex structure with many subunits and the interactions between these subunits. In other words, the cell is a complex nonlinear system composed of the interaction of many variables. On the other hand, the cell is an open system that constantly interacts with its environment, as it is out of thermodynamic equilibrium. In this respect, the cell can be defined as a 'complex non-equilibrium system'. In order to fulfill its basic functions, the cell maintains the non-equilibrium distribution of ions inside and outside the membrane [42].

Membrane currents result from movements of ions across cell membrane that are driven by electrochemical gradients. Depending on this, intracellular and extracellular distribution of ions is constantly changing as temporal [1,43,44]. The electrical activity of a cell depends on the number, variety and conductivity of ion channels. Many studies have been carried out to show that electrical conductivity disorders in ion channels cause various diseases. Therefore, conductivity measurement of ion channels is widely used. However, since the 'conductivity of the ion channel' is a fixed number obtained in the current–voltage ratio, it does not give detailed information about the electrical behavior of the cell. In the present study, time dependent entropy measurement methods are used to analyze cell behavior (or dynamics) over voltage variations [42]. The entropy of the cell changes over time depending on the change in the charge- concentration distributions of the ions inside and outside the cell. The entropy measures are a tool based on the probability distribution [26,33–35]. Therefore, the entropy is sensitive tool that can be used in detecting behavior varies of membrane currents. We used the windowed scalogram entropy method to observe the temporal change in the entropy of membrane currents.

The cell membrane, containing a wide distribution of ion channels, is a cellular structure targeted by nanoparticles. When nanoparticles come into contact with ion channels, they can either block the ion channels or alter the ion channel kinetics, affecting the physiological processes of the cell [5]. Therefore, direct or indirect interactions between

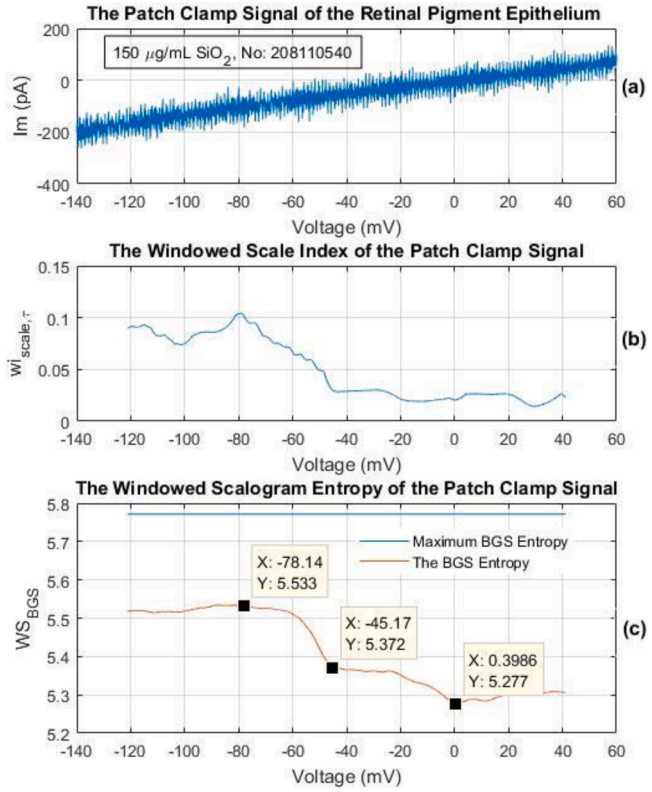

Fig. 18. The WndSI and WndSE for the patch clamp signal of the retinal pigment epithelium cell with registration number 208110540 in the 150 μM SiO_2 group. The windowed scalograms of the patch clamp signal were calculated for the time radius $\tau = 600$ time steps and the 'Morlet wavelet function' in the scale range $[s_0 = 8, s_1 = 256]$. **(a)** The patch clamp signal of a retinal pigment epithelium cell obtained by increasing the potential from −140 mV to +60 mV as temporal, for the SiO_2 dose of 150 μM **(b)** The WndSI spectrum indicates the temporal evolution of the non-periodicity degree of the patch clamp signal. **(c)** The WndSE spectrum indicates the temporal evolution of the BGS entropy of the patch clamp signal.

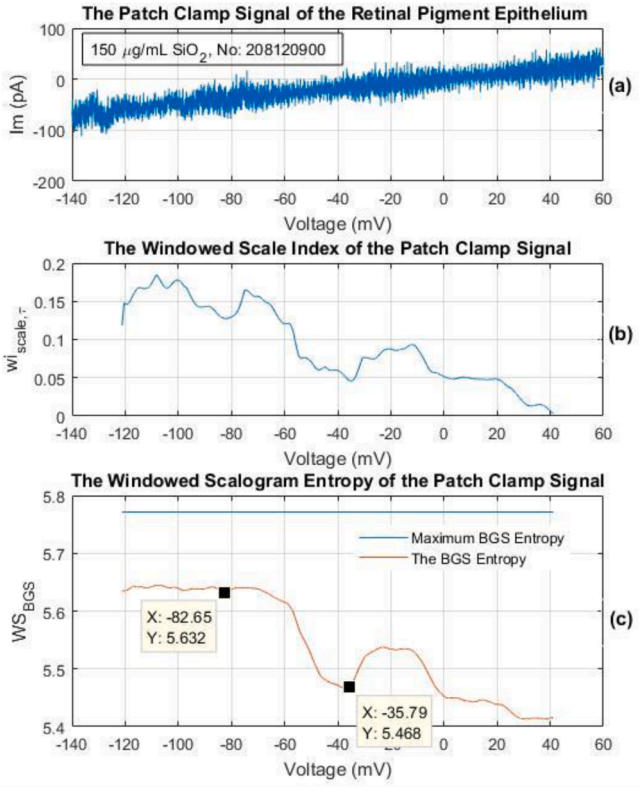

Fig. 19. The WndSI and WndSE for the patch clamp signal of the retinal pigment epithelium cell with registration number 208120900 in the 150 μM SiO_2 group. The windowed scalograms of the patch clamp signal were calculated for the time radius $\tau = 600$ time steps and the 'Morlet wavelet function' in the scale range $[s_0 = 8, s_1 = 256]$. **(a)** The patch clamp signal of a retinal pigment epithelium cell obtained by increasing the potential from −140 mV to +60 mV as temporal, for the SiO_2 dose of 150 μM **(b)** The WndSI spectrum indicates the temporal evolution of the non-periodicity degree of the patch clamp signal. **(c)** The WndSE spectrum indicates the temporal evolution of the BGS entropy of the patch clamp signal.

nanoparticles and ion channels are unavoidable. TRP channels are non-selective cationic transmembrane ion channels. These channels are responsible for a variety of sensory reactions and play important roles in regulating many physiological processes [5]. TRP channels mediating the leak Ca2+ entry to the RPE may be involved in basal cellular processes controlled by [Ca2+]i [24]. In this study, we investigated the effect of silica nanoparticles on RPE cell TRP currents by the entropy measure. In result section, figures show the temporal evolution graphs of entropy calculated for TRP currents of RPE cells recorded by increasing the ramp potential from −140 mV to +60 mV. Our findings showed that entropy changes depending on the voltage. When entropy versus voltage graphs are analyzed, significant differences between the TRP current signals of RPE cells exposed to SiO_2 nanoparticles and control can be observed. According to our results, the WS entropy values of RPE cells exposed to SiO_2 nanoparticles increase compared to the control group for voltage values lower than −40 mV. On the other hand, the application of SiO_2 nanoparticles to RPE cells shifted the minimum entropy to more positive voltages.

As known, the entropy of vivacity is lower than its surroundings. They keep their low entropy to continue their lives. Because, it is impossible for life to emerge in a state of equilibrium with a high entropy [45,46]. The results in figures are consistent with this general hypothesis that the retinal pigment epithelium cells survive by maintaining their low-entropy levels relative to maximum entropy. These results confirm our hypothesis that recorded of ion channel currents can be analyzed by non-linear methods other than classical methods (for example measurement of ion channel conductivity) to determine the nanoparticle-ion channel interaction.

Here, we conclude that the SiO_2 nanoparticles affect the electrical activity of the RPE cells. When we consider those findings, they indicate that the WndSE can be used to estimate the effects of nanoparticles on the membrane current. The use of this method is not limited to detecting the effect of SiO_2 nanoparticles on retinal pigment epithelial cells. The method can be used to analyze the interaction of different types of nanoparticles with ion channels. Morover the confirmation of our hypothesis in this study revealed that non-linear methods are a suitable method to study cell behavior caused by potential changes.

Funding

This work was supported by the Research Fund of Mersin University in Turkey under Grant (Number: 2019-1-TP2-3470).

Consent statement/Ethical approval: Not required.

Declaration of Competing Interest

The authors declare that they have no known competing financial interests or personal relationships that could have appeared to influence the work reported in this paper.

Table 1
For RPE cells, the windowed scalogram (WS) entropies values of TRP ion current signals at certain voltages in Figs. 2(c)–19(c). Also the mean and standard deviation (sd.) values of the WS entropies of TRP ion current signals at all voltages.

Control Group	Mean ± Sd	−100 mV	−80 mV	−60 mV	−40 mV	−20 mV	0 mV	20 mV	40 mV
Fig. 2	5.385 ± 0.059	5.307	5.304	5.409	5.46	5.454	5.387	5.399	5.357
Fig. 3	5.487 ± 0.064	5.399	5.418	5.567	5.558	5.553	5.52	5.468	5.407
Fig. 4	5.384 ± 0.028	5.326	5.366	5.393	5.441	5.402	5.387	5.388	5.389
Fig. 5	5.471 ± 0.031	5.468	5.475	5.553	5.444	5.447	5.455	5.471	5.459
Fig. 6	5.532 ± 0.036	5.557	5.568	5.548	5.54	5.52	5.526	5.457	5.483
Mean ± Sd	5.452 ± 0.065	5.411 ± 0.103	5.426 ± 0.101	5.494 ± 0.085	5.488 ± 0.056	5.475 ± 0.061	5.455 ± 0.068	5.436 ± 0.04	5.419 ± 0.051
50 μg/mL SiO_2 RPE	**Mean ± Sd**	**−100 mV**	**−80 mV**	**−60 mV**	**−40 mV**	**−20 mV**	**0 mV**	**20 mV**	**40 mV**
Fig. 7	5.581 ± 0.041	5.616	5.615	5.645	5.521	5.558	5.53	5.561	5.535
Fig. 8	5.558 ± 0.045	5.605	5.6	5.603	5.52	5.498	5.496	5.556	5.55
Fig. 9	5.526 ± 0.051	5.59	5.585	5.57	5.486	5.497	5.509	5.473	5.457
Fig. 10	5.477 ± 0.059	5.522	5.52	5.533	5.36	5.397	5.45	5.487	5.516
Fig. 11	5.428 ± 0.054	5.492	5.489	5.498	5.392	5.4	5.358	5.385	5.406
Mean ± Sd	5.514 ± 0.062	5.565 ± 0.055	5.562 ± 0.054	5.57 ± 0.057	5.456 ± 0.075	5.47 ± 0.07	5.468 ± 0.068	5.492 ± 0.072	5.493 ± 0.06
100 μg/mL SiO_2 RPE	**Mean ± Sd**	**−100 mV**	**−80 mV**	**−60 mV**	**−40 mV**	**−20 mV**	**0 mV**	**20 mV**	**40 mV**
Fig. 12	5.415 ± 0.054	5.434	5.364	5.437	5.47	5.473	5.398	5.336	5.309
Fig. 13	5.502 ± 0.025	5.519	5.552	5.525	5.484	5.492	5.49	5.475	5.49
Fig. 14	5.515 ± 0.025	5.537	5.543	5.523	5.483	5.501	5.516	5.497	5.462
Fig. 15	5.487 ± 0.065	5.399	5.401	5.525	5.462	5.526	5.547	5.534	5.492
Mean ± Sd	5.48 ± 0.045	5.472 ± 0.066	5.465 ± 0.096	5.503 ± 0.043	5.475 ± 0.106	5.498 ± 0.022	5.487 ± 0.064	5.461 ± 0.086	5.438 ± 0.087
150 μg/mL SiO_2 RPE	**Mean ± Sd**	**−100 mV**	**−80 mV**	**−60 mV**	**−40 mV**	**−20 mV**	**0 mV**	**20 mV**	**40 mV**
Fig. 16	5.427 ± 0.067	5.427	5.392	5.414	5.499	5.497	5.325	5.308	5.294
Fig. 17	5.455 ± 0.037	5.416	5.45	5.465	5.485	5.482	5.453	5.472	5.487
Fig. 18	5.409 ± 0.009	5.518	5.534	5.511	5.366	5.352	5.277	5.3	5.307
Fig. 19	5.541 ± 0.085	5.639	5.637	5.615	5.471	5.534	5.453	5.439	5.415
Mean ± Sd	5.458 ± 0.058	5.5 ± 0.103	5.503 ± 0.106	5.501 ± 0.085	5.455 ± 0.061	5.466 ± 0.079	5.377 ± 0.09	5.38 ± 0.088	5.375 ± 0.092

Table 2
The general summary of the windowed scalogram (WS) entropy values (of Table 1).

WS Entropy	Mean ± Sd	−100 mV Mean ± Sd	−80 mV Mean ± Sd	−60 mV Mean ± Sd	−40 mV Mean ± Sd	−20 mV Mean ± Sd	0 mV Mean ± Sd	20 mV Mean ± Sd	40 mV Mean ± Sd
Control Group	5.452 ± 0.065	5.411 ± 0.103	5.426 ± 0.101	5.494 ± 0.085	5.488 ± 0.056	5.475 ± 0.061	5.455 ± 0.068	5.436 ± 0.04	5.419 ± 0.051
SiO_2 RPE	5.486 ± 0.057	5.516 ± 0.081	5.514 ± 0.089	5.528 ± 0.068	5.461 ± 0.054	5.477 ± 0.059	5.446 ± 0.084	5.448 ± 0.089	5.44 ± 0.088

References

[1] Kulbacka J, Choromanska A, Rossowska J, Wezgowiec J, Saczko J, Rols MP. Cell Membrane Transport Mechanisms: Ion Channels and Electrical Properties of Cell Membranes. Adv Anat Embryol Cell Biol 2017;227:39–58.

[2] Borm PJ, Robbins D, Haubold S, et al. The potential risks of nanomaterials: a review carried out for ECETOC. Part Fibre Toxicol 2006;3:11.

[3] Yu P, Li J, Jiang J, et al. A dual role of transient receptor potential melastatin 2 channel in cytotoxicity induced by silica nanoparticles. Sci Rep 2015;5:18171.

[4] Sukhanova A, Bozrova S, Sokolov P, Berestovoy M, Karaulov A, Nabiev I. Dependence of Nanoparticle Toxicity on Their Physical and Chemical Properties. Nanoscale Res Lett 2018;13.

[5] Yin SH, Liu J, Kang YY, Lin YQ, Li DJ, Shao LQ. Interactions of nanomaterials with ion channels and related mechanisms. Brit J Pharmacol 2019;176:3754–74.

[6] Piscopo S, Brown ER. Zinc oxide nanoparticles and voltage- gated human Kv 11.1 potassium channels interact through a novel mechanism. Small 2018;14:e1703403.

[7] Gonzalez-Durruthy M, Werhli AV, Seus V, et al. Decrypting strong and weak single-walled carbon nanotubes interactions with mitochondrial voltage-dependent anion channels using molecular docking and perturbation theory. Scientific Rep 2017;7:13271.

[8] Calvaresi M, Furini S, Domene C, Bottoni A, Zerbetto F. Blocking the passage: C60 geometrically clogs K+ channels. ACS Nano 2015;9:4827–34.

[9] Russ KA, Elvati P, Parsonage TL, et al. C-60 fullerene localization and membrane interactions in RAW 264.7 immortalized mouse macrophages. Nanoscale 2016;8:4134–44.

[10] Mohammadpour R, Yazdimamaghani M, Reilly CA, Ghandehari H. Transient Receptor Potential Ion Channel-Dependent Toxicity of Silica Nanoparticles and Poly(amido amine) Dendrimers. J Pharmacol Exp Ther 2019;370:751–60.

[11] Yang X, Liu J, He H, et al. SiO2 nanoparticles induce cytotoxicity and protein expression alteration in HaCaT cells. Part Fibre Toxicol 2010;7:1.
[12] Chen Z, Meng H, Xing G, et al. Age-related differences in pulmonary and cardiovascular responses to SiO2 nanoparticle inhalation: nanotoxicity has susceptible population. Environ Sci Technol 2008;42:8985–92.
[13] Battal D, Celik A, Guler G, et al. SiO2 Nanoparticule-induced size-dependent genotoxicity - an in vitro study using sister chromatid exchange, micronucleus and comet assay. Drug Chem Toxicol 2015;38:196–204.
[14] Balli E, Comelekoglu U, Yalin S, et al. Toxic effects of silica nanoparticles on heart: electrophysiological, biochemical, histological and genotoxic study. Fresen Environ Bull 2016:612–22.
[15] McCarthy J, Inkielewicz-Stepniak I, Corbalan JJ, Radomski MW. Mechanisms of toxicity of amorphous silica nanoparticles on human lung submucosal cells in vitro: protective effects of fisetin. Chem Res Toxicol 2012;25:2227–35.
[16] Długosz O, Szostak K, Staroń A, Pulit-Prociak J, Banach M. Methods for reducing the toxicity of metal and metal oxide NPs as biomedicine. Materials 2020;13:279.
[17] Boulton M, Dayhaw-Barker P. The role of the retinal pigment epithelium: topographical variation and ageing changes. Eye 2001;15:384–9.
[18] Lakkaraju A, Umapathy A, Tan LX, et al. The cell biology of the retinal pigment epithelium. Prog Retin Eye Res 2020;78:100846.
[19] Yang S, Zhou J, Li D. Functions and Diseases of the Retinal Pigment Epithelium. Front Pharmacol 2021;12:727870.
[20] Sparrow JR, Hicks D, Hamel CP. The retinal pigment epithelium in health and disease. Curr Mol Med 2010;10:802–23.
[21] Ran J, Zhou J. Targeting the photoreceptor cilium for the treatment of retinal diseases. Acta Pharmacol Sin 2020;41:1410–5.
[22] Fukuoka Y, Strainic M, Medof ME. Differential cytokine expression of human retinal pigment epithelial cells in response to stimulation by C5a. Clin Exp Immunol 2003;131:248–53.
[23] Streilein JW, Ma N, Wenkel H, Ng TF, Zamiri P. Immunobiology and privilege of neuronal retina and pigment epithelium transplants. Vision Res 2002;42:487–95.
[24] Wimmers S, Strauss O. Basal calcium entry in retinal pigment epithelial cells is mediated by TRPC channels. Invest Ophthalmol Vis Sci 2007;48:5767–72.
[25] Beisbart CH. Probabilities in physics. Oxford University Press; 2011.
[26] Xiong W, Faes L, Ivanov PC. Entropy measures, entropy estimators, and their performance in quantifying complex dynamics: Effects of artifacts, nonstationarity, and long-range correlations. Phys Rev E 2017;95:062114.
[27] Stefanowicz-Hajduk J, Ochocka JR. Real-time cell analysis system in cytotoxicity applications: Usefulness and comparison with tetrazolium salt assays. Toxicol Rep 2020;7:335–44.
[28] Asada SS, Salih KM, Yassenc NY. Cytotoxic effect of silica nanoparticle on some tumor cell lines. JUPPAS 2018;26:206–13.
[29] Ahamed M. Silica nanoparticles-induced cytotoxicity, oxidative stress and apoptosis in cultured A431 and A549 cells. Hum Exp Toxicol 2013;32(2):186–95.
[30] Wang F, Gao F, Lan M, Yuan H, et al. Oxidative stress contributes to silica nanoparticle-induced cytotoxicity in human embryonic kidney cells. Toxicol In Vitro 2009;23:808–15.
[31] Song M, Chen D, Yu SP. The TRPC channel blocker SKF 96365 inhibits glioblastoma cell growth by enhancing reverse mode of the Na(+) /Ca(2+) exchanger and increasing intracellular Ca(2+). Br J Pharmacol 2014;71:3432–47.
[32] Reichhart N, Keckeis S, Fried F, et al. Regulation of surface expression of TRPV2 channels in the retinal pigment epithelium. Graefes Arch Clin Exp Ophthalmol 2015;253:865–74.
[33] Shannon CE. The mathematical theory of communication. MD Comput 1963;14 (1997):306–17.
[34] Gibbs JW. Elementary principles in statistical mechanics developed with especial reference to the rational foundation of thermodynamics. New York: C Scribner; 1902.
[35] O. Penrose, Foundations of statistical mechanics. Rep Prog Phys 1979;42:1937.
[36] Gray RM. Entropy and information theory. Springer Science & Business Media; 2011.
[37] Mallat SA. wavelet tour of signal processing. Elsevier; 1999.
[38] Benítez R, Bolós VJ, Ramírez ME. A wavelet-based tool for studying non-periodicity. Comput Math Appl 2010;60:634–41.
[39] Akıllı M, Yılmaz N. Windowed scalogram entropy: wavelet-based tool to analyze the temporal change of entropy of a time series. EPJ Plus 2021;136:1–14. https://doi.org/10.1140/epjp/s13360-021-02148-7.
[40] Bolós VB, Ferrer R, Jammazi R. The windowed scalogram difference: a novel wavelet tool for comparing time series. Appl Mat Comput 2017;312:49–65.
[41] Bolós VJ, Benítez R, Ferrer R. A New Wavelet Tool to Quantify Non-Periodicity of Non-Stationary Economic Time Series. Mathematics 2020;8:844.
[42] Akıllı M. Investıgatıon of tumor cell features by nonlınear methods [M.Sc. thesis]. İstanbul University-Cerrahpaşa Institute of Graduate Studies; 2022.
[43] Franco R, Bortner CD, Cidlowski JA. Potential roles of electrogenic ion transport and plasma membrane depolarization in apoptosis. J Membr Biol 2006;209:43–58.
[44] Sperelakis N. Cell physiology sourcebook: a molecular approach. Elsevier; 2001.
[45] Himeoka H, Kaneko K. Entropy production of a steady-growth cell with catalytic reactions. Phys Rev E 2014;90:042714.
[46] Shannon E. What is life? The physical aspect of the living cell. At the University Press; 1951.